

Volodymyr REBROV, Vladimir LUKIN

National Aerospace University “Kharkiv Aviation Institute”, Kharkiv, Ukraine

POST-PROCESSING OF COMPRESSED NOISY IMAGES USING BM3D FILTER

Acquired images are often noisy. Since the amount of such images increases, they should be compressed where lossy compression is often applied for several reasons. Such compression is associated with the phenomena of specific image filtering due to lossy compression and the possible existence of an optimal operation point (OOP). However, such filtering is not perfect, and residual noise can be quite intensive even if an image is compressed at the so-called optimal operation point. Then, additional post-filtering can be applied. Thus, the basic **subject** of this paper is the post-processing of noisy images compressed in a lossy manner. The main **goal** of this paper is to consider the possible application of a block-matching 3-dimensional (BM3D) filter to images corrupted by additive white Gaussian noise compressed by a better portable graphics (BPG) coder with a compression ratio smaller than that for the optimal operation point and in OOP neighborhood. The **tasks** of this paper are to analyze the efficiency of compressed image post-processing depending on noise intensity, image complexity, coder compression parameter Q , and filter threshold parameter β according to different quality metrics and to provide practical recommendations on setting the filter and coder parameters. The main **result** is that the post-processing efficiency decreases when the coder compression parameter increases and becomes negligible for a coder compression parameter slightly larger than its value for OOP. The post-processing efficiency is larger for simpler structure images and larger noise intensity. Compressed image quality due to post-processing improves according to the standard criterion peak signal-to-noise ratio and visual quality metrics. For larger coder compression parameters, the optimal threshold shifts toward smaller values. In conclusion, we demonstrate the efficiency of post-processing and show that the BM3D filter outperforms the standard discrete cosine-based (DCT) filter. We also provide recommendations for filter parameter setting. We also outline possible research directions for the future.

Keywords: lossy compression; noisy images; coders; quality metrics; post-filtering.

1. Introduction

Nowadays images are acquired by numerous types of imaging systems and are employed in agriculture [1, 2], technology [3, 4], medicine [5, 6], and everyday life [7]. As the number of acquired images steadily grows, there is also a stable tendency for the image average size to increase. Therefore, there is a necessity for efficient image compression for their transfer via communication lines and storage. There exist lossless [8] and lossy [9, 10] image compression methods.

Lossless compression does not introduce losses into compressed images, but the compression ratio (CR) is often inappropriate. Therefore, lossy compression techniques have been widely applied. Because they introduce losses, a trade-off between the compressed image quality [11], CR, and other characteristics should be reached [12, 13]. Visual quality can be considered [11, 14], image classification [15, 16], and object detection aspects can be important [17].

In many practical situations, it is assumed (or it is supposed by default) that the images to be compressed are noise-free [9, 14]. Then, rate-distortion curves have monotonous behavior, and using them, it is possible to provide a desired CR or a desired quality (according to a

given metric) or an appropriate trade-off between them [12, 14]. Meanwhile, there are many practical situations where images to be compressed are corrupted by noise [18, 19]. This occurs for optical [19] and medical [4] images obtained under complex conditions as well as for synthetic aperture radar images [2]. Lossy compression in this case has certain specific features [20, 21]. The first is a specific noise filtering effect (although it is less than the denoising effect of conventional filtering of noisy images) [20, 22]. The second is the possible existence of the so-called optimal operation point, i.e., such a value of the parameter that controls compression (PCC) for a given encoder that the compressed image is maximally close to the corresponding noise-free one according to a chosen quality (similarity) metric [23]. Lossy compression in the optimal operation point (OOP), if it exists, has two advantages. First, a rather high CR, which is considerably larger than that for lossless compression, is usually provided. Second, the compressed image quality is higher than that for uncompressed noisy images. If OOP does not exist, then a more “careful” lossy compression is recommended [23].

Recently, it has been shown that compressed noisy images can be efficiently post-processed to additionally improve their quality [24, 25]. For this purpose, a discrete

cosine transform (DCT) based filter [24, 26] has been applied to noisy images compressed by a better portable graphics (BPG) coder [27], which is one of the best modern coders. The following has been demonstrated. First, post-filtering can efficiently improve image quality, especially for Q (that serves as PCC for the BPG-coder) smaller than Q that corresponds to OOP (Q_{OOP}) and for images of relatively simple structure corrupted by intensive noise. Second, the DCT-based filter properties can be varied by a parameter β used in the threshold setting; optimal values of this parameter can be found, and the general tendency is that optimal β decreases if Q becomes larger, image complexity increases, and noise intensity reduces.

Meanwhile, the DCT-based filter is not the best [28]. In particular, the block-matching 3-dimensional (BM3D) filter [28] can perform better in traditional denoising applications according to both conventional and visual quality metrics. This allows the expectation that the BM3D filter can efficiently cope with residual noise in the post-processing of lossy compressed noisy images.

Thus, the goal of this paper is to analyze the BM3D applicability for removing the residual noise in noisy images compressed by the BPG coder. If its efficiency is confirmed, then the secondary goal is to propose how to set the filter parameters optimally.

The paper is organized as follows. The problem of denoising lossy compressed noisy images is refreshed in Section 2. Preliminary analysis of BM3D filter applicability to post-processing is performed in Section 3. A more detailed analysis results are presented in Section 4 and discussed in Section 5. Finally, the Conclusions follow.

2. Problem statement and existing approaches

2.1. Problem statement

From the very beginning, let us describe our image/noise model and the requirements for processing such images, where lossy compression is the main step. Suppose we have an image corrupted by additive white Gaussian noise (AWGN):

$$I_{ij}^n = I_{ij}^{\text{true}} + n_{ij}, \quad (1)$$

where I_{ij}^n is the noisy ij -th pixel value, I_{ij}^{true} denotes the true ij -th pixel value, and n_{ij} is the noise. It is assumed that AWGN has zero mean and variance σ^2 that is known in advance or accurately pre-estimated by some known blind method [29, 30]. Note that we start by considering the AWGN model for two reasons. First, it is the model often used in studies dealing with image

denoising [26, 28] and lossy compression of noisy images [21, 23]. Second, before studying more complex noise models, it is worth considering the AWGN model as a starting point. Note also that, in simulations and preliminary studies, we assume having the true image and adding the noise artificially. In other words, we have three images: the true, noisy, and compressed ($\{I_{ij}^c, i = 1, \dots, I; j = 1, \dots, J\}$) ones where I and J define the image size. If the compressed image is post-filtered, then we also have also the image $\{I_{ij}^{\text{pf}}, i = 1, \dots, I; j = 1, \dots, J\}$. In fact, we have to compare the quality of noisy, compressed, and post-filtered images and other parameters for them (e.g., CR, computational efficiency of their obtaining) to understand the best strategy. Here we mean that the following strategies are possible:

- 1) to have the original (noisy, uncompressed or compressed in a lossless manner) image;
- 2) to obtain the image compressed with a certain Q ;
- 3) to obtain the image compressed with a certain Q and then post-processed with a certain filter and certain parameters of this filter.

In our preliminary analysis, we need test images and criteria for their quality. Usually, in analysis, at least two images of different complexity are employed, where one should have a quite simple structure and the second has to be rather complex. Similar to [24], we use the simple structure image Frisco (Fig. 1, a) and the complex structure image Fr03 (Fig. 1, b), both of which are grayscale.

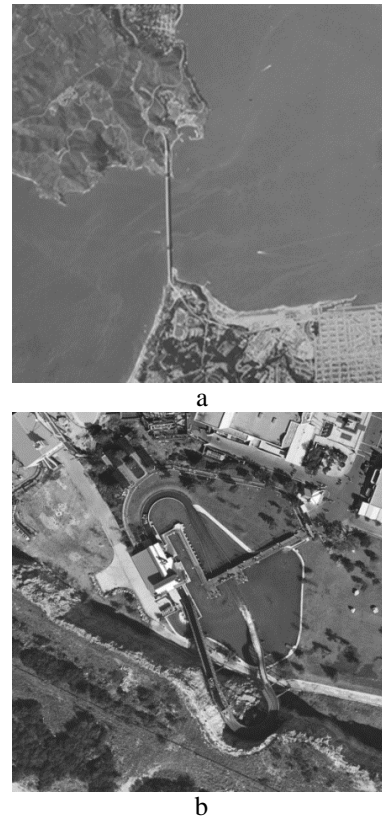


Fig. 1. Two grayscale test images of different complexity used in our study: Frisco (a) and Fr03 (b)

Since we have the true image $I_{\square}^{\text{true}}$ that can be treated as a reference, the quality of images I_{\square}^{n} , I_{\square}^{c} , and I_{\square}^{pf} can be determined using full-reference metrics (quantitative criteria). Let us use the peak signal-to-noise ratio (PSNR) for the beginning. Fig. 2 presents three images: I_{\square}^{n} for $\sigma^2 = 100$ (Fig. 2, a), I_{\square}^{c} for $Q=27$, where Q is the parameter that controls compression (PCC) for the BPG coder (Fig. 2, b), and the results of its post-processing by the DCT-based filter with the hard threshold $T = 2.3\sigma_{\square}^2$, i. e. $\beta = 2.3$ (Fig. 2, c).



Fig. 2. Noisy ($\sigma^2 = 100$) (a), compressed ($Q=27$) (b), and DCT-filtered ($\beta = 2.3$) (c) images

As one can see, noise for the image in Fig. 2, a is visible, especially in homogeneous regions (PSNR=28.1 dB; recall that for PSNR<35 dB the distortions are usually visible). Lossless compression of this image is almost useless since CR is only slightly larger than unity (e.g., for Zip it equals to 1.005 and, for Rar, CR= 1.003). Compression with $Q=27$ (Fig. 2, b) leads to PSNR=28.27 dB and CR=3.22, i.e. to the better quality of the compressed image compared to the noisy image quality (according to PSNR metric) and considerably better CR. A small noise-filtering effect is observed. Finally, the post-filtering leads to even considerably better result. Clearly, the CR is the same as in the previous case (post-filtering is applied to decompressed images) but the quality after decompression is significantly better (PSNR=37.22 dB).

Interesting dependence describing the peculiarities of lossy compression of noisy images are shown in Figures 3 and 4. Here we show the improvement or degradation of image quality depending on CR, where a larger CR corresponds to a larger Q (although dependences of CR on Q are very individual and are greatly influenced by image and noise properties). The improvement or degradation is expressed as

$$\delta\text{PSNR}_{\text{cn}}(Q) = \text{PSNR}_{\text{c}}(Q) - \text{PSNR}_{\text{n}} , \quad (2)$$

$$\delta\text{PSNR}_{\text{pfm}}(Q) = \text{PSNR}_{\text{pf}}(Q) - \text{PSNR}_{\text{n}} , \quad (3)$$

where PSNR_{n} , $\text{PSNR}_{\text{c}}(Q)$, and $\text{PSNR}_{\text{pf}}(Q)$ are PSNR values for noisy, compressed, and post-filtered images, respectively; the latter two are functions of Q .

Let us start by considering the dependence for the image Fr03. The dependence $\delta\text{PSNR}_{\text{cn}}(Q)$ start from approximately 0 for CR about 3 and then behaves in a slightly different manner depending on noise variance. For $\sigma^2 = 50$ (Fig. 3,a), there is a maximum observed for a CR of approximately 9, then $\delta\text{PSNR}_{\text{cn}}(Q)$ monotonically decreases with Q increasing. Moreover, the values of $\delta\text{PSNR}_{\text{cn}}(Q)$ become negative, i.e., the compressed image quality is worse than the noisy image quality. For $\sigma^2 = 100$ (Fig. 3,b) and $\sigma^2 = 200$ (Fig. 3,c), there are obvious maxima of $\delta\text{PSNR}_{\text{cn}}(Q)$ observed for CR \approx 12 and CR \approx 18, respectively. These are optimal operation points that occur for

$$Q_{\text{OOP}} = 15+20\lg(\sigma), \quad (4)$$

i.e. $Q_{\text{OOP}}=35$ for $\sigma^2 = 100$ and $Q_{\text{OOP}}=38$ for $\sigma^2 = 200$ [24]. Expression (4) means that the probable OOP position can be determined under the condition of known or accurately pre-estimated noise standard deviation. The results in [23] demonstrate that the existence of OOP for a given noisy image can be predicted with high accuracy.

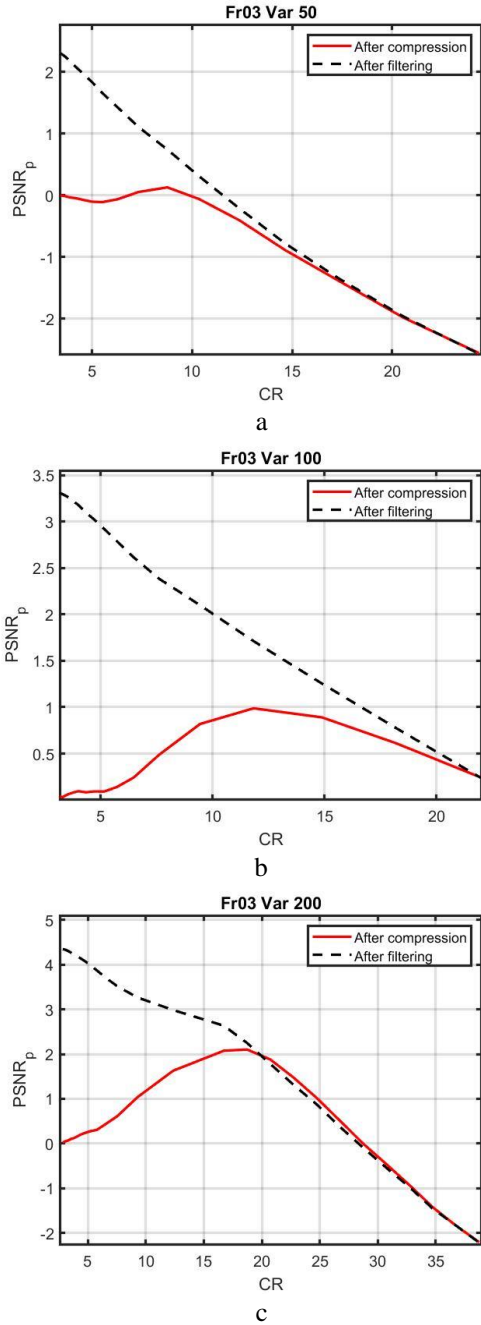


Fig. 3. Dependences for the test image Fr03 for noise variance equal to 50 (a), 100 (b), and 200 (c)

This means that one can decide whether it is worth compressing an image with Q_{OOP} (4) before the execution of lossy compression or not.

It is worth noting here that dependence $\delta PSNR_{pfn}(Q)$ has been obtained under the assumption that optimal β (that corresponds to maximal PSNR of post-processed image) is used.

This dependence is monotonically decreasing irrespective of the noise variance. The analysis shows the following:

1) $\delta PSNR_{pfn}(Q)$ is the largest for small CR (and, respectively, small Q) when the compressed image is

very close to the noisy one and efficient post-processing (filtering of residual noise) is possible; for larger CR (and Q), residual noise becomes less intensive and its suppression is less efficient;

2) the positive effect due to post-processing can be quite large; it exceeds 2 dB for $\sigma^2 = 50$, 3 dB for $\sigma^2 = 100$, and 4 dB for $\sigma^2 = 200$;

3) if CR approximately corresponds to Q_{OOP} , the efficiency of post-processing is not large, it is about 0.6 dB; after this, for larger CR (and Q), post-processing becomes useless.

Analysis of data for the test image Frisco (Fig. 4) shows the following:

1) the main conclusions coincide with those given above;

2) the difference is that the effect of post-processing characterized by $\delta PSNR_{pfn}(Q) - \delta PSNR_{cn}(Q)$ is larger: it exceeds 8 dB for $\sigma^2 = 50$, 9 dB for $\sigma^2 = 100$, and 10 dB for $\sigma^2 = 200$; this is not surprising because, as known [19, 26, 28], the filtering efficiency depends on noise intensity and image complexity, which are higher for less complex images and greater intensity of the noise.

It is also worth mentioning the tendency that optimal β for the DCT-based filter decreases if Q increases.

2.2. Possible solution

In this paper, we analyze the coder and the filters that are among the best assuming that their combination produces the best outcomes (in general, different compression techniques can be applied to noisy images [27, 31] and different filters can be used for post-processing [32]). The BPG coder has the following advantage: it has considerably better performance compared to JPEG and outperforms many modern coders, the BPG encoder is easy to use (its CCP Q can be only integer and varies in the limits from 1 to 51 (a larger Q leads to a higher CR and worse visual quality in compressing noise-free images)). The BPG coder can process images presented in different formats with 8–14 bits. These were the reasons for our interest in the BPG coder.

The filters that belong to the DCT-based family (<https://webpages.tuni.fi/foi/>) are attractive because of several important properties. First, DCT is a good data decorrelation transform approaching Karhunen-Loeve one. Second, there are versions of the DCT-based filters for different types of noise, including signal-dependent and spatially correlated ones that either use variance-stabilizing transforms or adapt threshold calculation algorithms to a noise type [33]. Third, the texture-preserving property of DCT-based filters is worth admitting [33]. Finally, the DCT-based filter properties can be varied and optimized according to different criteria due to the possibility of varying parameters such as the block size,

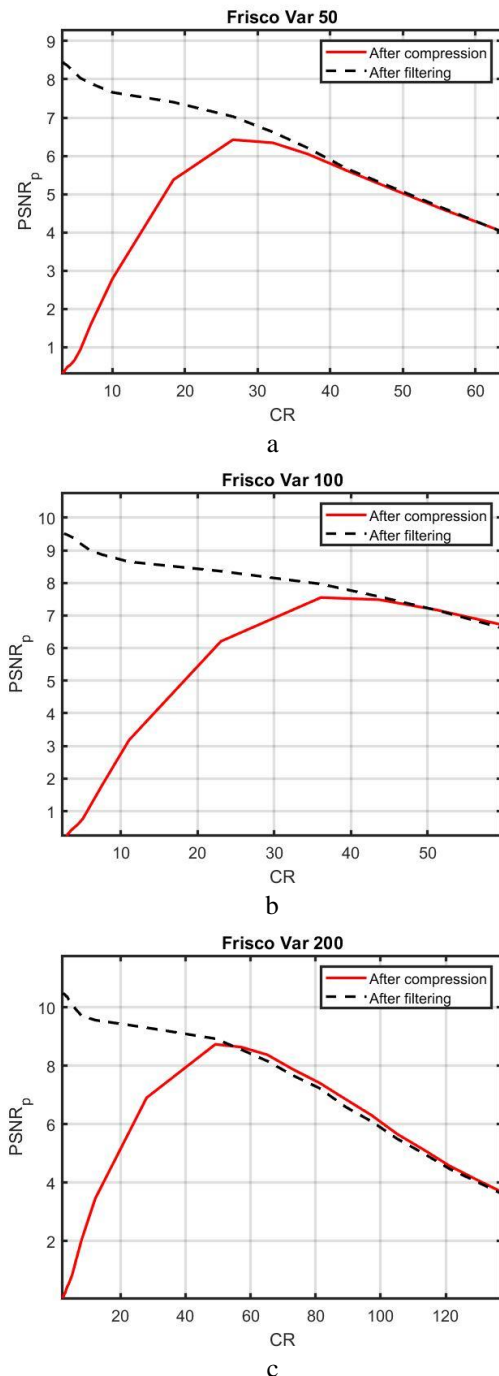


Fig. 4. Dependences for the test image Frisco for noise variance equal to 50 (a), 100 (b), and 200 (c)

threshold type, and aforementioned parameter β . While the default setting of β for hard threshold is 2.7 ($T=2.7\sigma$), it is possible to decrease β to provide better edge/detail/texture preservation or better visual quality. Recall here that if the DCT-based filter is applied after lossy compression of a noisy image, we have a standard deviation of residual noise $\sigma_{res} < \sigma$ and, thus, the threshold should be smaller. Because we do not estimate σ_{res} after lossy compression, threshold reduction should be

performed by diminishing β to provide quasi-optimal performance of the filter.

The BM3D filter is the most advanced version of the DCT-based filters. It exploits not only the positive features of the DCT, but also the non-local approach [19, 28] that presumes the search for similar patches (blocks) and their joint denoising. Due to these modifications, the BM3D filter usually provides a higher output PSNR than the standard DCT filter with fully overlapping 8×8 pixel blocks and a hard threshold. In addition, the BM3D filter is characterized by better visual quality of output images due to better edge/detail/texture preservation. Finally, similar to the standard DCT-based filter, it is possible to manipulate the filter properties by varying β . These are the main reasons for our expectation that the BM3D filter can be efficient for the considered application.

3. Preliminary analysis of the BM3D filter applicability

First, let us check whether or not the positive effect of post-filtering occurs and whether there is dependence of post-processing efficiency on β , σ , and Q . For this purpose, we obtained dependences $PSNR_{pf}(\beta)$ for fixed $\sigma^2 = 100$ and several values of Q in the range from 28 to 40. Some of them for the test image Fr03 are presented in Fig. 5. Recall that $Q=36$ approximately corresponds to optimal operation point.

The main tendencies are the same as those observed for the standard DCT-based coder. First, for Q equal to 28, 32, and 36, there are obvious maxima for β that shift toward smaller values of β if Q increases. Meanwhile, there is no maximum for $PSNR_{pf}(\beta)$ if $Q=40$, i.e. if $Q > Q_{OOP}$. In addition, the values of $PSNR_{pf}(\beta)$ are smaller than $PSNR_n$, i.e., the quality of compressed and processed images is lower than that of noisy images. Post-processing is thus useless.

The maximum value of $PSNR_{pf}(\beta)$ decreases if Q increases. It equals 31.5 dB for $Q=28$, to 31.0 dB for $Q=32$, and 29.9 dB for $Q=36$. This means that the BM3D filter performs well and can be used in post-processing. However, the post-processing efficiency significantly depends on Q .

Fig. 6 presents four dependences $PSNR_{pf}(\beta)$ for fixed $\sigma^2 = 100$ for the other test image. As one can see, the main tendencies are the same. The only difference is in the maximal values of $PSNR_{pf}(\beta)$ that are considerably larger than those for the test image Fr03. The reason is that the test image Frisco has a simpler structure and, thus, can be denoised better.

We are also interested in whether BM3D produce any benefits compared to the standard DCT-based filter? To partly answer this question, let us analyze data given in Table 1.

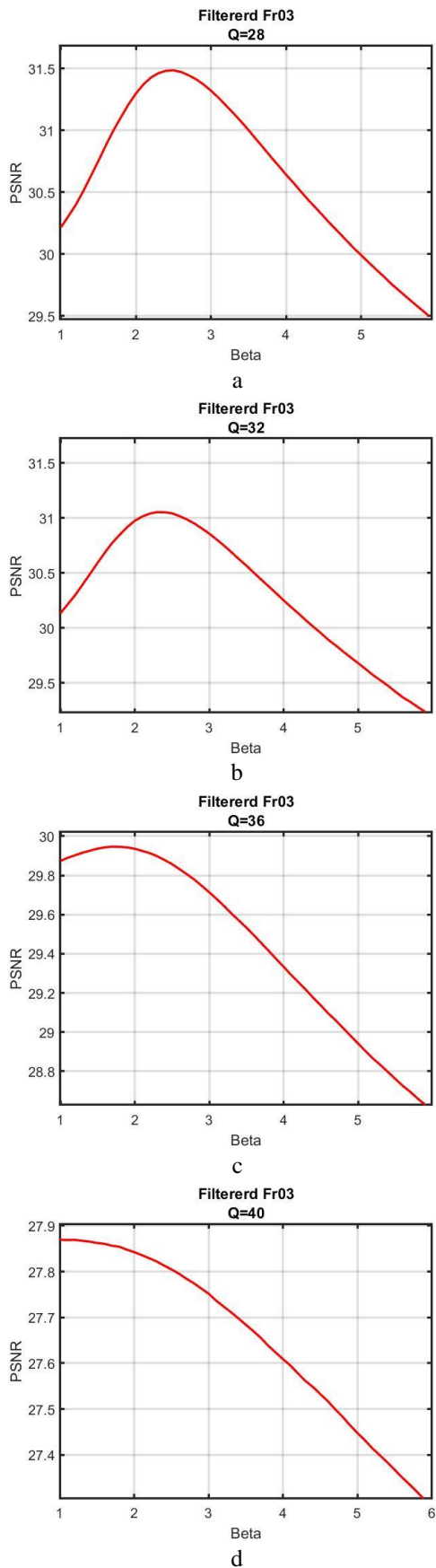


Fig. 5. $PSNR_{pf}(\beta)$ for fixed $\sigma^2 = 100$ and values of Q equal to 28 (a), 32 (b), 36 (c), and 40, image Fr03

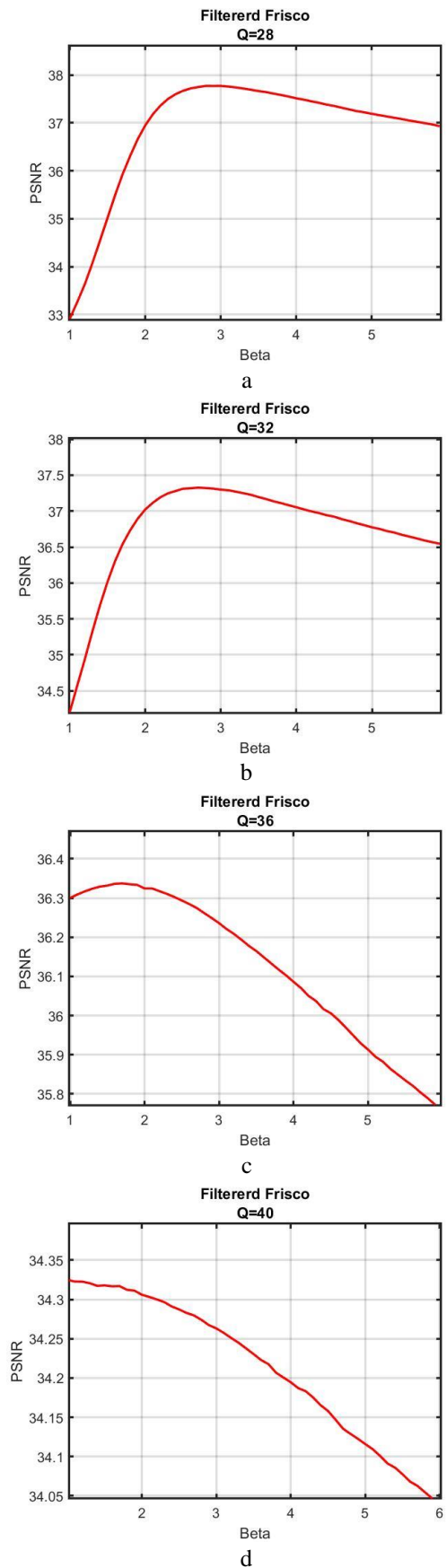


Fig. 6. $PSNR_{pf}(\beta)$ for fixed $\sigma^2 = 100$ and values of Q equal to 28 (a), 32 (b), 36 (c), and 40, image Frisco

Table 1
Comparison of BM3D and standard DCT-based filters,
 $\sigma^2 = 100$, the test image Frisco

Q	Standard DCT filter		BM3D filter	
	β_{opt}	PSNR _m	β_{opt}	PSNR _m
24	2.8	37.45	3.0	37.93
25	2.8	37.44	3.0	37.90
26	2.8	37.42	2.9	37.86
27	2.8	37.39	2.8	37.82
28	2.7	37.35	2.8	37.77
29	2.7	37.31	2.8	37.70
30	2.7	37.21	2.8	37.60
31	2.6	37.12	2.8	37.48
32	2.6	37.01	2.7	37.32
33	2.5	36.93	2.7	37.17
34	2.3	36.80	2.4	36.97
35	2.0	36.62	2.2	36.68
36	1.8	36.27	1.7	36.33
37	1.6	35.89	1.6	35.95
38	1.6	35.43	1.5	35.48
39	1.4	34.87	1.4	34.90
40	1.4	34.30	1.0	34.32

Here we present the values of β_{opt} and maximal PSNR_{pf} (in dB) attained for β_{opt} . As seen, the values of β_{opt} for both filters are practically the same for a given Q.

If Q is considerably smaller than Q_{OOB} (35 for the considered case), the optimal values of β practically do not change and are close to the optimal values recommended for conventional denoising applications. However, starting from $Q \approx Q_{OOB} - 5$, β_{opt} starts to decrease and is about 2.1 for $Q \approx Q_{OOB}$.

The values of PSNR_m are different for the considered filters if $Q \leq Q_{OOB}$. The largest difference is observed for $Q < Q_{OOB} - 5$ and it reaches approximately 0.5 dB. This means that the BM3D filter is preferable.

Similar studies have been carried out for $\sigma^2 = 50$ and $\sigma^2 = 200$ as well as for the test image Fr03 for all three values of the noise variance. Very similar results were obtained. The observed tendency is that the benefits of the BM3D filter compared with the standard DCT-based filter are larger for larger noise variance and simpler structure images.

4. Detailed analysis

First, analysis of PSNR_{pf}(β, Q) can be performed using three-dimensional representations of these functions. Fig. 7 shows two examples. They demonstrate two main tendencies:

- maximal values decrease if Q increases;
- β_{opt} reduces if Q becomes larger.

The metric PSNR is not the best in characterizing the visual quality of original and/or processed images

[34]. Therefore, many other (visual quality) metrics have been proposed in recent years. Therefore, let us use one of them, namely PSNR-HVS-M (<https://ponomarenko.info/psnrhvs.htm>) in our analysis (where HVS relates to human vision system and M to masking).

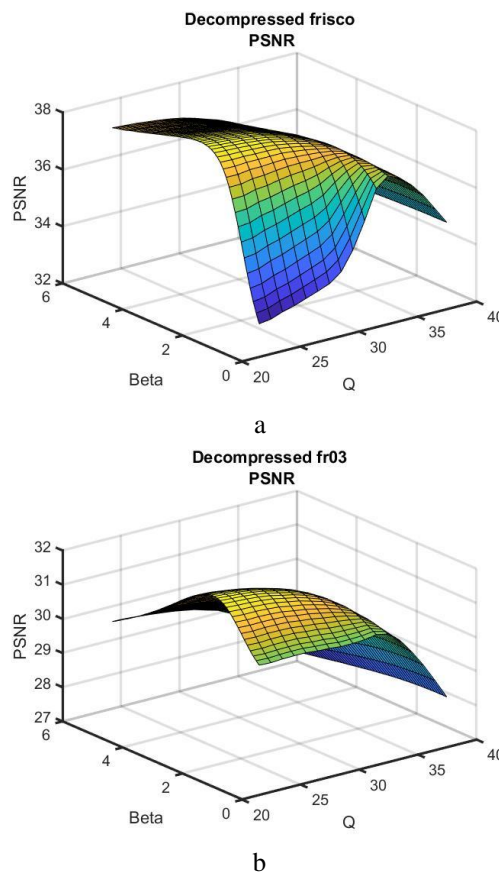


Fig. 7. 3D representations of PSNR_{pf}(β, Q) for $\sigma^2 = 100$ for the decompressed test images Frisco (a) and Fr03 (b) after post-processing by the BM3D filter

This metric considers two important properties of the human vision system (HVS): less sensitivity to distortions in higher spatial frequencies than in low spatial frequencies and masking effect. In our case, it is also important that PSNR-HVS-M can be applied to grayscale images. Its values are larger than the corresponding PSNR if noise (distortions) is white and an essential masking effect occurs. In contrast, PSNR-HVS-M is smaller than PSNR if the distortions are close to spatially correlated noise and the masking effect is practically absent. PSNR-HVS-M is expressed in dB, where its larger values correspond to a better visual quality. PSNR-HVS-M corresponds to practically invisible distortions if its value exceeds 41 dB.

Fig. 8 presents dependence PSNR – HVS – M_{pf}(β) obtained for $\sigma^2 = 100$ and four values of Q (28, 32, 36, and 40) for the test image Fr03. The plots are similar to the corresponding plots in Fig. 5.

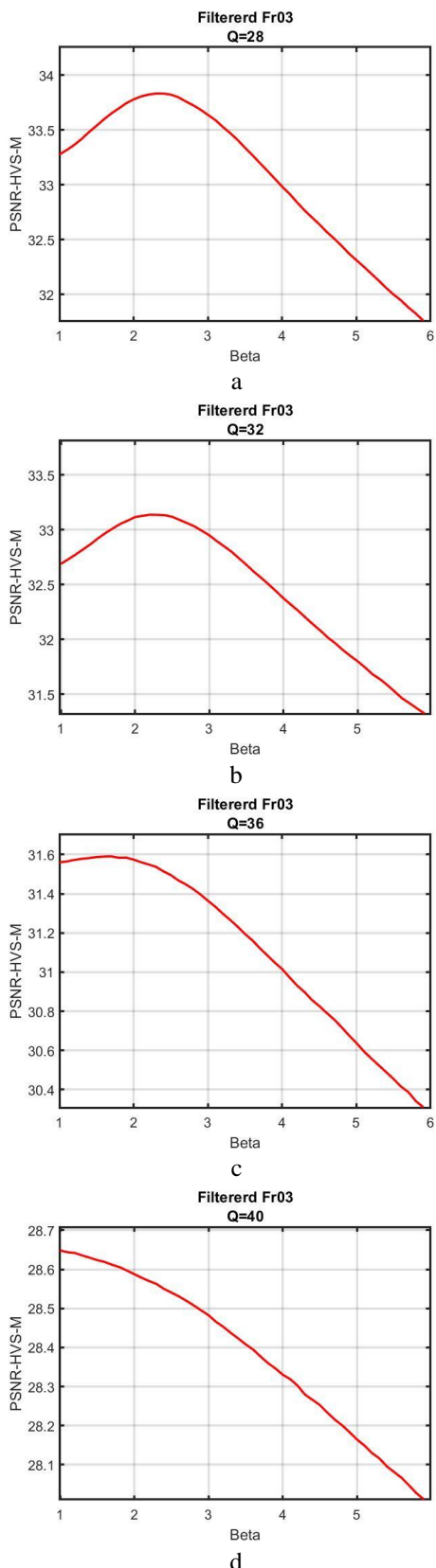


Fig. 8. PSNR – HVS – $M_{pf}(\beta)$ for fixed $\sigma^2 = 100$ and values of Q equal to 28 (a), 32 (b), 36 (c), and 40 (d), image Fr03

Again, there are obvious maxima for $Q=28$ and 32 (Figures 8, a and 8, b, respectively) observed for β_{opt} of

about 2.3. Meanwhile, for $Q = 36 \approx Q_{OOP}$, the maximum exists but its value (31.6 dB) is significantly smaller than that for $Q = 28$ (33.8 dB) and $Q = 32$ (33.2 dB). Besides, β_{opt} for $Q = 36$ has shifted to 1.7.

This means that post-processing is efficient and worth applying for $Q \approx Q_{OOP}-3$. For larger Q, post-processing efficiency decreases rapidly as Q grows.

Fig. 9 shows the dependence PSNR – HVS – $M_{pf}(\beta)$ obtained for $\sigma^2 = 100$ and four values of Q (28, 32, 36, and 40) for the test image Frisco. The first observation is that the dependence is similar to the corresponding dependence PSNR $_{pf}(\beta)$ in Fig. 6 as well as dependences PSNR – HVS – $M_{pf}(\beta)$ in Fig. 8 for the other test image. The specific features are as follows. First, larger maximal values are provided than those for the corresponding data in Fig. 8. This approach deals with less complexity of the image Frisco and, thus, better efficiency of its lossy compression and denoising. Second, for the same Q and β , PSNR – HVS – M_{pf} values are, in general, larger for the test image Frisco. Meanwhile, the conclusion is the same – it is not worth compressing images with $Q > Q_{OOP}$ where Q_{OOP} is described by expression (4) and it is useless to perform post-processing in this case. In fact, compression with $Q > Q_{OOP}$ can be reasonable (used) only if for Q_{OOP} a desired CR is not produced.

We are also interested in whether the BM3D filter produces a better visual quality of post-processed images compared to the standard DCT-based filter. For this purpose, the data for the metric PSNR – HVS – M_{pf} have been collected and are presented in Table 2. As seen, BM3D shows better performance for $Q \leq Q_{OOP}-3$. Then, the difference reduces and, for $Q \geq Q_{OOP}$, post-processing by any of the considered filters becomes useless.

The cases of other test images and other values of noise variance have also been studied. The observed tendencies and conclusions are the same as above. The benefit of using the BM3D filter is greater for simpler structure images (Frisco in our case) and for larger noise intensity. For $Q \leq Q_{OOP}-3$, it is possible to recommend using $\beta_{opt}=2.3$ to provide the best visual quality.

5. Discussion

The analysis of the simulation data shows the following. The proposed approach can be helpful when images subject to compression are contaminated by intensive noise. This often occurs in radar [2] and ultrasound medical [4] imaging as well as for optical images acquired under poor illumination conditions [15]. Since the positive effect of post-filtering can be sufficiently large (PSNR and PSNR-HVS-M can be improved by several dB), it is worth providing the post-filtering option for systems that deal with processing of images of the aforementioned types where lossy compression is needed.

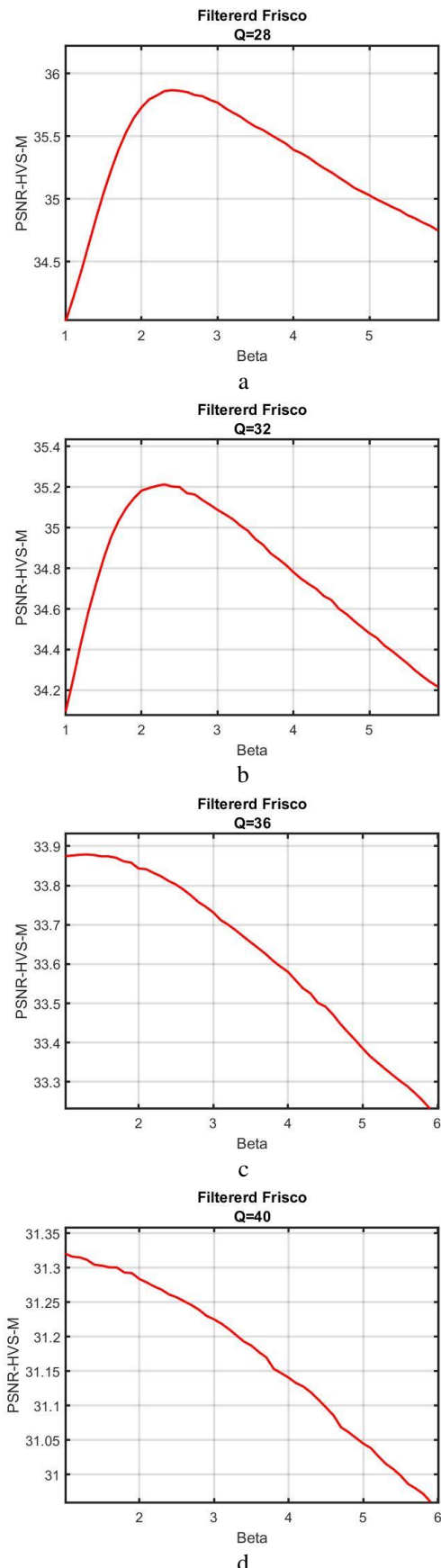


Fig. 9. PSNR – HVS – $M_{pr}(\beta)$ for fixed $\sigma^2 = 100$ and values of Q equal to 28 (a), 32 (b), 36 (c), and 40 (d), image Frisco

Table 2

Comparison of the BM3D and standard DCT-based filters, $\sigma^2 = 100$, the test image Frisco, PSNR-HVS-M

Q	Standard DCT filter		BM3D filter	
	β_{opt}	PSNR _m	β_{opt}	PSNR _m
24	2.5	35.66	2.5	36.11
25	2.5	35.64	2.5	36.08
26	2.5	35.59	2.5	36.00
27	2.5	35.53	2.5	35.93
28	2.5	35.48	2.4	35.86
29	2.4	35.40	2.3	35.79
30	2.4	35.25	2.3	35.62
31	2.4	35.14	2.3	35.47
32	2.3	34.92	2.3	35.21
33	2.2	34.77	2.3	34.98
34	2.1	34.59	2.1	34.72
35	1.9	34.33	2.0	34.31
36	1.6	33.84	1.3	33.87
37	1.5	33.36	1.3	33.41
38	1.4	32.81	1.1	32.87
39	1.2	32.09	1.0	32.11
40	1.1	31.30	1.0	31.32

The proposed method has several limitations and should be further advanced. The principal limitation is that it is useless for $Q \geq Q_{OOP}$. Denoising based on trained neural networks [6] may be helpful, but we have doubts because statistics of residual noise are very complex.

Another problem deals with the simplified noise model used in our design. AWGN model is approximately adequate for optical imaging, but noise in radar and medical images is usually signal dependent. However, it is possible to overcome this problem by applying a proper variance stabilizing transform [25] before compression and/or denoising. One more problematic point with AWGN model is that noise can be spatially correlated. This case requires additional studies.

One more assumption put into the basis of our design is that noise statistics is known in advance. In this sense, we can state that there exist blind methods that can perform estimation of noise properties accurately enough [29].

Our studies have also shown that post-filtering performance depends on image complexity. This means that image and noise properties have to be incorporated into the decision of whether it is worth performing post-filtering of compressed noisy images and what should be the filter parameters.

6. Conclusions

In this paper, we have considered the problem of post-processing noisy images compressed in a lossy manner by the BPG coder. It is shown that post-processing

can be efficient under the following conditions:

- a) the parameter that controls compression is smaller than Q_{OOP} determined by (4);
- b) noise intensity is quite high;
- c) image complexity is not large;
- d) an efficient filter is applied;
- e) its parameters are adapted to the properties of residual noise.

It is demonstrated that the BM3D filter with an optimal threshold is more efficient than the standard DCT-based filter for the PCC $Q \leq Q_{OOP}-3$ in terms of conventional and visual quality metrics. The difference according to PSNR can reach 0.5 dB and such a difference could be expected from other studies dealing with denoising efficiency. If the computational efficiency of post-filtering is not of prime importance, the use of the BM3D filter with the recommended threshold parameter is expedient.

For the PCC $Q \geq Q_{OOP}$, the post-filtering is practically useless. This recommendation can be incorporated in automatic multistage processing of noisy images if there are some restrictions on the provided CR.

The basic limitations of the proposed approach and used AWGN model have been discussed. In the future, it will be reasonable to consider other types of noise and some other types of filters. Multichannel images are also worth considering. It is also worth using visual quality metrics that consider human vision attention (saliency maps) [35, 36].

Contributions of authors: conceptualization – **Vladimir Lukin**; methodology – **Vladimir Lukin**; formulation of tasks – **Vladimir Lukin**; analysis – **Volodymyr Rebrov**; development of model – **Volodymyr Rebrov**; software – **Volodymyr Rebrov**; verification – **Volodymyr Rebrov**; analysis of results – **Vladimir Lukin, Volodymyr Rebrov**; visualization – **Volodymyr Rebrov**; writing – **Volodymyr Rebrov**; writing – review and editing – **Vladimir Lukin**.

All the authors have read and agreed to the published version of this manuscript.

References

1. Kussul, N., Lavreniuk, M., Shelestov, A., & Skakun, S. Crop inventory at regional scale in Ukraine: Developing in season and end of season crop maps with multi-temporal optical and SAR satellite imagery. *European Journal of Remote Sensing*, 2018, vol. 51, no. 1, pp. 627-636. DOI: 10.1080/22797254.2018.1454265.
2. Fang, J., Mao, T., Bo, F., Hao, B., Zhang, N., Hu, S., Lu, W., & Wang, X. A SAR Image-Despeckling Method Based on HOSVD Using Tensor Patches. *Remote Sensing*, 2023, vol. 15, article no. 3118. DOI: 10.3390/rs15123118.
3. Ma, Y., Wu, H., Wang, L., Huang, B., Ranjan, R., Zomaya, A., & Jie, W. Remote sensing big data computing: Challenges and opportunities. *Future Generation Computer Systems*, 2015, vol. 51, pp. 47-60. DOI: 10.1016/j.future.2014.10.029.
4. Lan, Y., & Zhang, X. Real-Time Ultrasound Image Despeckling Using Mixed-Attention Mechanism Based Residual UNet. *IEEE Access*, 2020, vol. 8, pp. 195327-195340. DOI: 10.1109/ACCESS.2020.3034230.
5. Heo, Y.-C., Kim, K., & Lee, Y. Image Denoising Using Non-Local Means (NLM) Approach in Magnetic Resonance (MR) Imaging: A Systematic Review. *Applied Sciences*, 2020, vol. 10, article no. 7028. DOI: 10.3390/app10207028.
6. Ponomarenko, M., Miroshnichenko, O., Lukin, V., Kryvenko, S., & Egiazarian, K. Blind denoising of dental X-Ray images. *Proceedings of SPIE EI Symposium*, 2023, vol. 35, pp. 299-1-299-6. DOI: 10.2352/EI.2023.35.9.IPAS-299.
7. Bataeva, E., & Chumakova-Sierova, A. Values in visual practices of Instagram network users. *Lecture Notes in Networks and Systems*, 2022, vol. 367, pp. 992-1002. DOI: 10.1007/978-3-030-94259-5_76
8. Hussain, A. J., Al-Fayadh, A., & Radi, N. Image compression techniques: A survey in lossless and lossy algorithms. *Neurocomputing*, 2018, vol. 300, pp. 44-69. DOI: 10.1016/j.neucom.2018.02.094.
9. Sayood, K. *Introduction to data compression*. San Francisco, Morgan Kaufmann Publ., 2017. 680 p. Available at: https://www.mbit.edu.in/wp-content/uploads/2020/05/data_compression.pdf (accessed 10.07.2023).
10. Blanes, I., Magli, E., & Serra-Sagrasta, J. A tutorial on image compression for optical space imaging Systems. *IEEE Geoscience and Remote Sensing Magazine*, 2014, vol. 2, no. 3, pp. 8-26, DOI: 10.1109/MGRS.2014.2352465.
11. Bondžulić, B., Stojanović, N., Petrović, V., Pavlović, B., & Miličević, Z. Efficient prediction of the first just noticeable difference point for JPEG compressed images. *Acta Polytechnica Hungarica*, 2021, vol. 18, no. 8, pp. 201-220. DOI: 10.12700/APH.18.8.2021.8.11.
12. Li, F., Krivenko, S., & Lukin, V. Two-step providing of desired quality in lossy image compression by SPIHT. *Radioelectronic and computer systems*, 2020, no. 2, pp. 22-32. DOI: 10.32620/reks.2020.2.02.
13. Jeong, Y. W., Yang, J. Y., Jung, Y. B., Jeon, B. W., Cha, S. H., Kang, S. J., & Dinh, Q. K. *Rate distortion optimization encoding system and method of operating the same*. Patent US, no. 10,742,995 B2. 2020. Available at: <https://patents.justia.com/patent/10742995> (accessed 10.07.2023).

14. Oh, H., Bilgin, A., & Marcellin, M. Visually lossless JPEG 2000 for remote image browsing. *Information*, 2016, vol. 7, no. 3, article no. 45. DOI: 10.3390/info7030045.
15. Zabala, A., Pons, X., Díaz-Delgado, R., Garcia, F., Auli-Llinas, F., & Serra-Sagrista, J. Effects of JPEG and JPEG2000 lossy compression on remote sensing image classification for mapping crops and forest areas. *Proceedings of 2006 IEEE International Symposium on Geoscience and Remote Sensing*, Denver, CO, USA, 2006, pp. 790-793. DOI: 10.1109/IGARSS.2006.203.
16. Ozah, N., & Kolokolova, A. Compression improves image classification accuracy. *Advances in Artificial Intelligence. Canadian AI 2019. Lecture Notes in Computer Science*, vol. 11489, Springer, Cham., 2019, pp. 525-530. DOI: 10.1007/978-3-030-18305-9_55.
17. Doss, S., Pal, S., Akila, D., Jeyalakshmi, S., Nusrat Jabeen, T., & Suseendran, G. Satellite image remote sensing for identifying aircraft using SPIHT and NSCT. *Journal of Critical Reviews*, 2020, vol. 7, no. 5, pp. 631-634. Available at: <https://jcreview.com/paper.php?slug=satellite-image-remote-sensing-for-identifying-aircraft-using-spiht-and-nsct> (accessed 10.07.2023).
18. Lim, S. H. Characterization of Noise in Digital Photographs for Image Processing. *Proceeding in Digital Photography II*, 2008, vol. 6069, pp. 219-228. DOI: 10.1117/12.655915.
19. Chatterjee, P., & Milanfar, P. Is Denoising Dead? *IEEE Transactions on Image Processing*, 2010, vol. 19, no. 4, pp. 895-911. DOI: 10.1109/TIP.2009.2037087.
20. Al-Chaykh, O. K., & Mersereau, R. M. Lossy compression of noisy images. *IEEE Transactions on Image Processing*, 1998, vol. 7, iss. 12, pp. 1641-1652. DOI: 10.1109/83.730376.
21. Chang, S. G., Yu, B., & Vetterli, M. Adaptive wavelet thresholding for image denoising and compression. *IEEE Trans. on Image Processing*, 2000, vol. 9, iss. 9, pp. 1532-1546. DOI: 10.1109/83.862633.
22. Yang, D., Lv, W., Zhang, J., Chen, H., Sun, X., Lv, S., Dai, X., Luo, R., Zhou, W., Qiu, J., & Shi, Y. Low-dose imaging denoising with one pair of noisy images. *Optics Express*, 2023, vol. 31, iss. 9, article no. 14159. DOI: 10.1364/OE.482856.
23. Kovalenko, B., Lukin, V., Kryvenko, S., Naumenko, V., & Vozel, B. BPG-Based Automatic Lossy Compression of Noisy Images with the Prediction of an Optimal Operation Existence and Its Parameters. *Applied Sciences*, 2022, vol. 12, iss. 15, article no. 7555. DOI: 10.3390/app12157555.
24. Kovalenko, B., Lukin, V., & Rebrov, V. Analysis of the potential efficiency of post-filtering noisy images after lossy compression. *Ukrainian journal of remote sensing*, 2023, vol. 10, no. 1, pp. 11-16. DOI: 10.36023/ujrs.2023.10.1.231.
25. Chen, X., Liu, L., Zhang, J., & Shao, W. Infrared image denoising based on the variance-stabilizing transform and the dual-domain filter. *Digital Signal Processing*, 2021, vol. 113, article no. 103012. DOI: 10.1016/j.dsp.2021.103012.
26. Fevrarev, D., Lukin, V., Ponomarenko, N., Abramov, S., Egiazarian, K., & Astola, J. Efficiency analysis of DCT-based filters for color image database. *SPIE Conference Image Processing: Algorithms and Systems IX*, 2011, vol. 7870. DOI: 10.1117/12.871944.
27. Bellard, F. *BPG Image format. Release 0.9.8*. Available at: <https://bellard.org/bpg/>. (accessed 10.07.2023).
28. Lebrun, M. An Analysis and Implementation of the BM3D Image Denoising Method. *Image Processing On Line*, 2012, vol. 2, pp. 175-213. DOI: 10.5201/ipol.2012.l-bm3d.
29. Colom, M., Buades, A., & Morel, J.-M. Nonparametric noise estimation method for raw images. *Journal of the Optical Society of America A*, 2014, vol. 31, no. 4, pp. 863-871. DOI: 10.1364/JOSAA.31.000863.
30. Selva, E., Kountouris, A., & Louet, Y. K-Means Based Blind Noise Variance Estimation. *IEEE 93rd Vehicular Technology Conference (VTC2021-Spring)*, Helsinki, Finland, 2021, pp. 1-7. DOI: 10.1109/VTC2021-Spring51267.2021.9449072.
31. Bekhtin, Y. S. Adaptive wavelet codec for noisy image compression, *9th East-West Design & Test Symposium (EWDTs)*, Sevastopol, Ukraine, 2011, pp. 184-188. DOI: 10.1109/EWDTs.2011.6116587.
32. Simmer, K. U., Bitzer, J., & Marro, C. Post-Filtering Techniques. In: *Brandstein, M., Ward, D. (eds) Microphone Arrays. Digital Signal Processing*, Springer, Berlin, Heidelberg, 2001, pp. 39-60. DOI: 10.1007/978-3-662-04619-7_3.
33. Rubel, O., Lukin, V., Krivenko, S., Pavlikov, V., Zhyla, S., & Tserne, E. Reduction of Spatially Correlated Speckle in Textured SAR Images. *International Journal of Computing*, 2021, vol. 20, no. 3, pp. 319-327. DOI: 10.47839/ijc.20.3.2276.
34. Lin, W., & Jay Kuo, C.-C. Perceptual visual quality metrics: A survey. *Journal of Visual Communication and Image Representation*, 2011, vol. 22, iss. 4, pp. 297-312. DOI: 10.1016/j.jvcir.2011.01.005.
35. Kim, C., & Milanfar, P. Visual saliency in noisy images. *Journal of Vision*, 2013, vol. 13, no. 4, article no. 5, pp. 1-14. DOI: 10.1167/13.4.5.
36. Lukin, V., Bataeva, E., & Abramov, S. Saliency map in image visual quality assessment and processing. *Radioelectronic and computer systems*, 2023, no. 1, pp. 112-121. DOI: 10.32620/reks.2023.1.09.

Received 07.09.2023, Accepted 20.11.2023

ПОСТ-ОБРОБКА СТИСНУТИХ ЗАШУМЛЕНИХ ЗОБРАЖЕНЬ ФІЛЬТРОМ ВМ3D

Володимир Ребров, Володимир Лукін

Отримані зображення часто бувають спотворені шумом. Оскільки кількість таких зображень збільшується, їх слід стискати і внаслідок кількох причин часто застосовується стиск із втратами. Таке стиснення пов'язане з ефектами специфічної фільтрації зображень внаслідок стиснення з втратами та можливим існуванням оптимальної робочої точки (ОРТ). Однак така фільтрація не є ідеальною, і залишковий шум може бути досить інтенсивним, навіть якщо зображення стискається в так званій оптимальній робочій точці. Для покращення якості зображення можна застосувати додаткову пост-фільтрацію. Таким чином, основним **предметом** статті є пост-обробка зашумлених зображень, стиснутих із втратами. Основна **мета** статті – розглянути можливість застосування тривимірного фільтра блочного зіставлення (ВМ3D) до зображень, спотворених адитивним білим гаусівським шумом, стиснутим кращим кодером better portable graphics (BPG) зі ступенем стиснення меншим, ніж для оптимальної робочої точки та в околиці ОРТ. **Завдання** даної статті — проаналізувати ефективність пост-обробки стиснених зображень залежно від інтенсивності шуму, складності зображення, параметра кодера Q, що керує стисненням, та параметра фільтра β , що визначає поріг, за різними метриками якості, дати практичні рекомендації щодо налаштування параметрів фільтра та кодера. Основний **результат** полягає в тому, що ефективність пост-обробки знижується зі збільшенням значення параметра, що керує стисненням (ПКС), і стає незначною для ПКС трохи більшого, ніж ПКС для ОРТ. Ефективність є вищою для зображень з більш простою структурою і більшою інтенсивністю шуму. Якість стисненого зображення за рахунок пост-обробки покращується відповідно до стандартного критерію пікового відношення сигнал-шум та за візуальними показниками якості. При більшому ПКС оптимальне значення порогу зміщується у бік менших значень. Як **висновки** продемонстровано ефективність пост-обробки та показано, що ВМ3D-фільтр працює краще, ніж стандартний ДКП-фільтр. Також надано рекомендації щодо налаштування параметрів фільтра. Також окреслені можливі напрямки досліджень на майбутнє.

Ключові слова: стиснення з втратами; зашумлені зображення; кодери; показники якості; пост-фільтрація.

Ребров Володимир Сергійович – асп. каф. інформаційно-комунікаційних технологій ім. О. О. Зеленського, Національний аерокосмічний університет ім. М. Є. Жуковського «Харківський авіаційний інститут», Харків, Україна.

Лукін Володимир Васильович – д-р техн. наук, проф., зав. каф. інформаційно-комунікаційних технологій ім. О. О. Зеленського, Національний аерокосмічний університет ім. М. Є. Жуковського «Харківський авіаційний інститут», Харків, Україна.

Volodymyr Rebrov – PhD Student of the Department of Information-Communication Technologies named after O. O. Zelensky, National Aerospace University "Kharkiv Aviation Institute", Kharkiv, Ukraine, e-mail: mr.vladimirrebrov@gmail.com, ORCID: 0000-0002-6442-3155.

Vladimir Lukin – Doctor of Technical Sciences, Professor, Head of the Department of Information-Communication Technologies named after O. O. Zelensky, National Aerospace University "Kharkiv Aviation Institute", Kharkiv, Ukraine, e-mail: lukin@ai.kharkov.com, ORCID: 0000-0002-1443-9685.